Outline

- Simulations of toroidicity-induced Alfvén eigenmode
  - The geometry in simulations and the theoretical model for TAE
  - TAE is obtained from simulations
  - Benchmark with eigemode calculation
  - Driving effect of energetic particles
  - Damping mechanisms
- Summary

Transport of energetic particles

- Typical energetic particle energy: E_{hot} > 100 kev >> T_{th}
  - Energetic particles heat plasmas via Coulomb collisions
  - Energetic particles can be introduced by Neutral Beam Injection (NBI heating) or by Ion Cyclotron Range of Frequency (ICRF) heating
  - As approaching ignition condition, a fusion reactor produces energetic particles:

$$D_1^2 + T_1^3 \rightarrow n_0^1 \text{ (14.1 MeV)} + He_2^4 \text{ (3.5 MeV)}$$

- Energetic particles will drive toroidicity-induced Alfven eigenmodes (TAEs) unstable
  - TAEs are MHD-scale modes
  - Unstable TAEs will transport energetic particles
  - The loss of energetic particles reduces the heating efficiency and damages the reactor device

Toroidicity-induced Alfvén eigenmodes

- Shear Alfvén wave dispersion relation in cylindrical geometry

$$\omega_A^2 = k_\parallel^2 V_A^2,\quad k_\parallel = \left(n - \frac{m}{q(r)}\right)/R,\quad V_A^2(\vec{r}) = \frac{B(\vec{r})^2}{n_0 m_i}$$

- Continuum spectra are broken and form a frequency gap due to the magnetic field variation in toroidal geometry

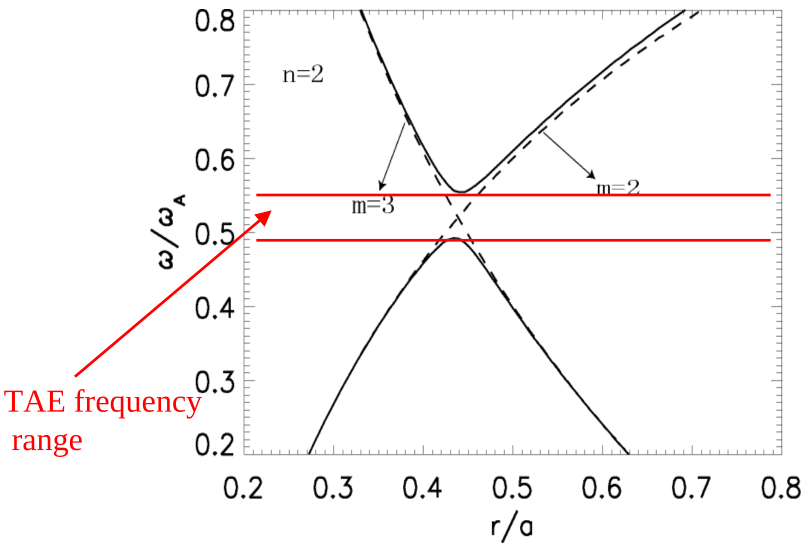

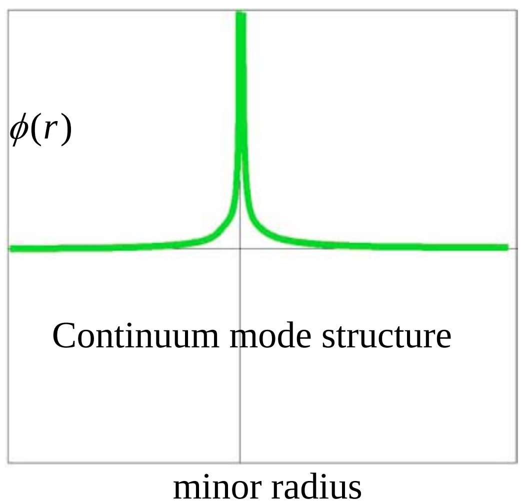

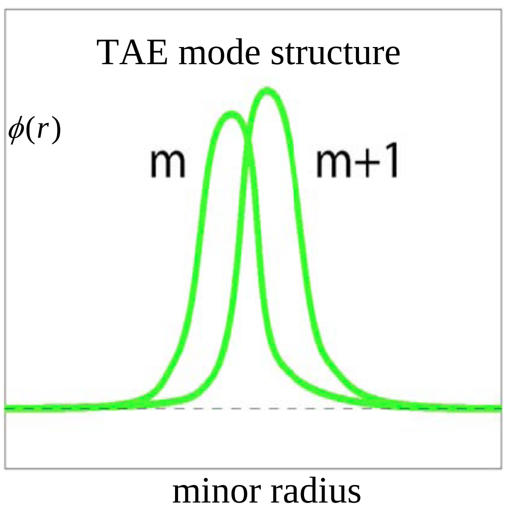

- Discrete global modes with frequencies located inside the gap—**TAEs**

The TAE simulations presented here use global geometry

- **Equilibrium quantities are determined by the Miller model**

R. L. Miller, et. al., Phys. Plasmas **5**, 973 (1998)

$$R(r,\theta) = R_0(r) + r\cos[\theta + \arcsin(\delta)\sin(\theta)]$$
$$Z(r,\theta) = \kappa r\sin(\theta)$$

- **Field-line-following coordinates**

$$x = r - r_0$$
$$y = \frac{r_0}{q_0}\left(\int_0^\theta \hat{q}(r,\theta)\,d\theta - \zeta\right)$$
$$z = q_0 R_{maj}\theta$$

- **Boundary conditions**

$$\phi(x=0,y,z) = \phi(x=l_x,y,z) = 0$$
$$\phi(x,y=0,z) = \phi(x,y=l_y,z)$$
$$\phi(x,y,z=0) = \phi(x,y,z=l_z)$$

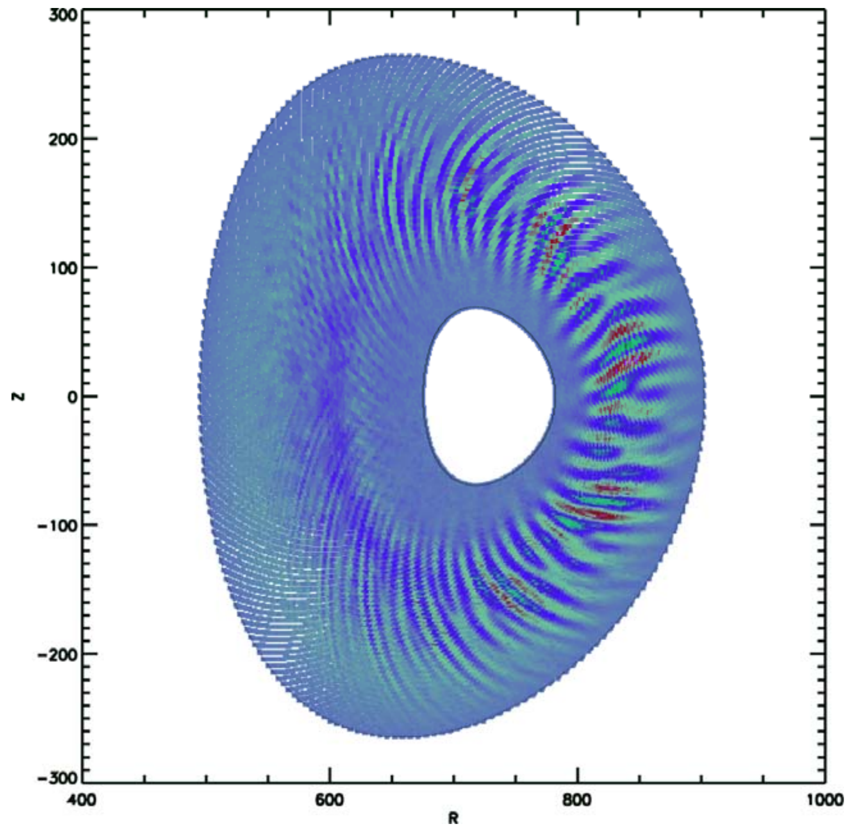

Y. Chen and S. Parker, *J. of Comp. Phys.* **220** 839 (2007)

Simulation parameters

- Basic parameters:

  $$B_0 = 1.91\,\mathrm{T},\ R_0 = 1.67\,m,\ a = 0.36 R_0$$

- Profile:

  $$q(r) = 1.3\left(\frac{r}{r_0}\right)^{0.3},\quad r_0 = a/2,\quad \hat{s}(r) = 0.3\left(\frac{r_0}{r}\right)^{0.7}$$

- Plasma to magnetic pressure ratio and mass ratio:

  $$\beta = 3.0\times 10^{-3},\ m_i / m_p = 2$$

- Simulation domain:

  $$[0.2a, 0.8a]$$

- External drive:

  Add external n=2 current for 200 steps, then observe the subsequent oscillation and mode structure

Simulation results

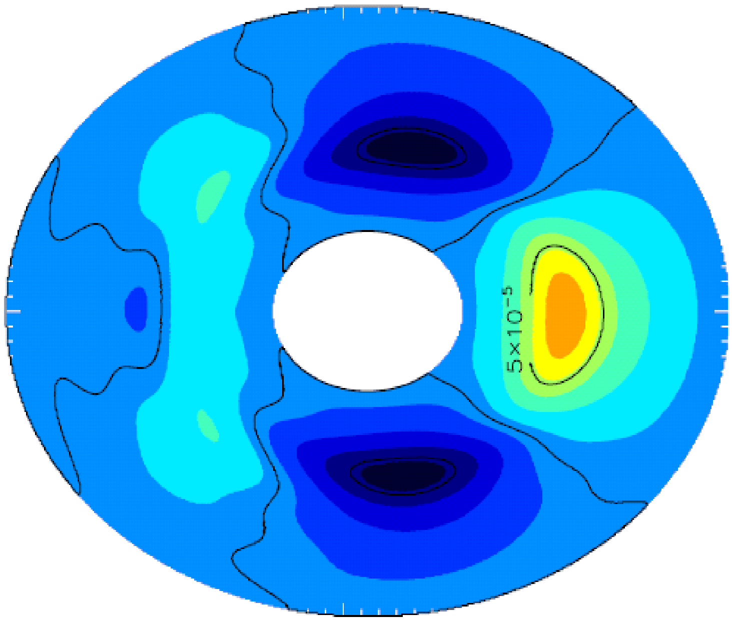

contour plot of electric potential from simulations

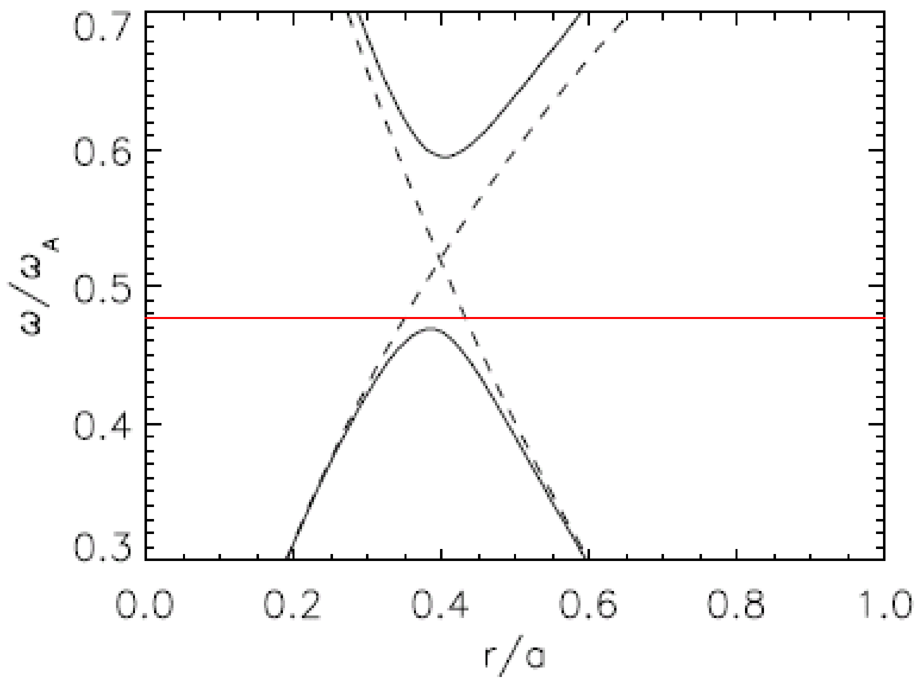

- Simulations assume fluid electrons
- The mode frequency falls in the gap predicted by Fu and Van dam (1989)
- The global mode structure is observed

The MHD equations for the shear Alfvén wave

- **Quasi-neutrality**

$$\boxed{-\nabla \frac{n_0 m_i}{B(\vec{r})^2} \nabla_\perp \phi = \delta n_i - \delta n_e}$$

- **Continuity equations**

$$\left.\begin{aligned} \frac{\partial \delta n_i}{\partial t} + n_0 \vec{B} \cdot \nabla \frac{u_{\|i}}{B} + \vec{E} \times \hat{b} \cdot \nabla n_0 &= 0 \\ \frac{\partial \delta n_e}{\partial t} + n_0 \vec{B} \cdot \nabla \frac{u_{\|e}}{B} + \vec{E} \times \hat{b} \cdot \nabla n_0 &= 0 \end{aligned}\right\}$$

$$\boxed{\frac{\partial}{\partial t}(\delta n_i - \delta n_e) + n_0 \vec{B} \cdot \nabla \frac{(u_{\|i} - u_{\|e})}{B} = 0}$$

- **Ampere's law**

$$\boxed{-\nabla_\perp{}^2 A_\| = \mu_0 q n_0 (u_{\|i} - u_{\|e})}$$

- **Faraday's law**

$$\boxed{\frac{\partial A_\|}{\partial t} + \hat{b} \cdot \nabla \phi = 0}$$

- **MHD TAE equation**

$$\boxed{\frac{\partial^2}{\partial t^2} \nabla \frac{1}{V_A(\vec{r})^2} \nabla_\perp \phi = \vec{B} \cdot \nabla \frac{1}{B} \nabla_\perp{}^2 \hat{b} \cdot \nabla \phi, \quad V_A(\vec{r}) = \frac{B(\vec{r})^2}{n_0 m_i}}$$

Benchmark with eigenmode calculation

- The simplified form: $$\vec{B}\cdot\nabla\frac{1}{B}\sim\hat{b}\cdot\nabla\ ,\quad \hat{b}\cdot\nabla\sim\frac{\partial}{\partial z}$$

  In simulations, continuity equation becomes: $$\frac{\partial}{\partial t}(\delta n_i-\delta n_e)+n_0\hat{b}\cdot\nabla(u_{\|i}-u_{\|e})=0$$

- Eigenmode calculation: $$\frac{1}{V_A^2}\frac{\partial^2}{\partial t^2}\nabla_\perp^2\phi=\hat{b}\cdot\nabla\nabla_\perp^2\hat{b}\cdot\nabla\phi$$

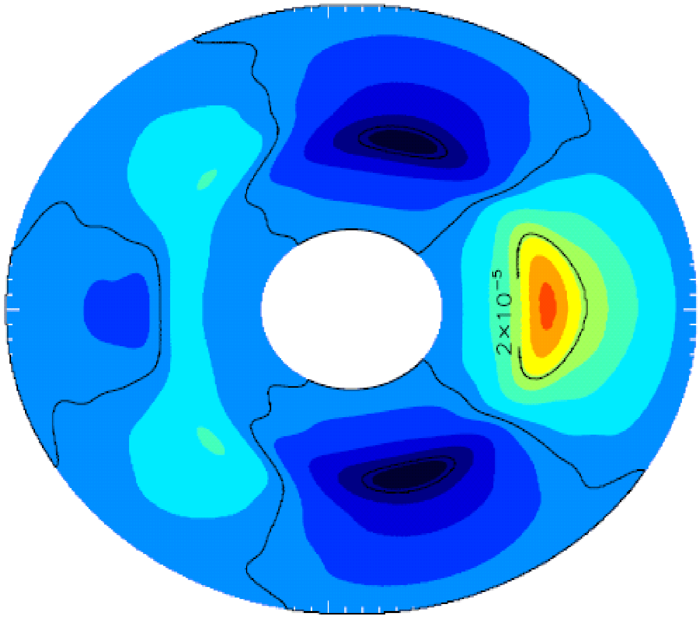

contour plot of electric potential from simulations

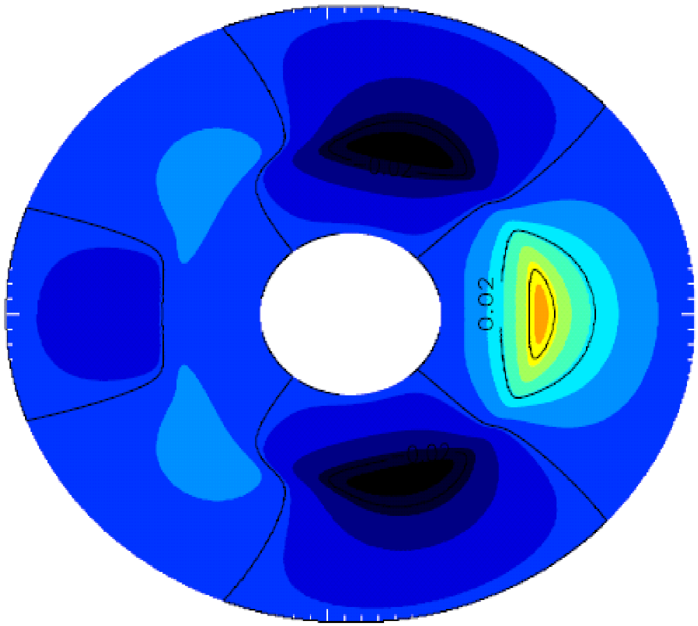

contour plot of electric potential from eigenmode calculation

Driving effect of energetic particles

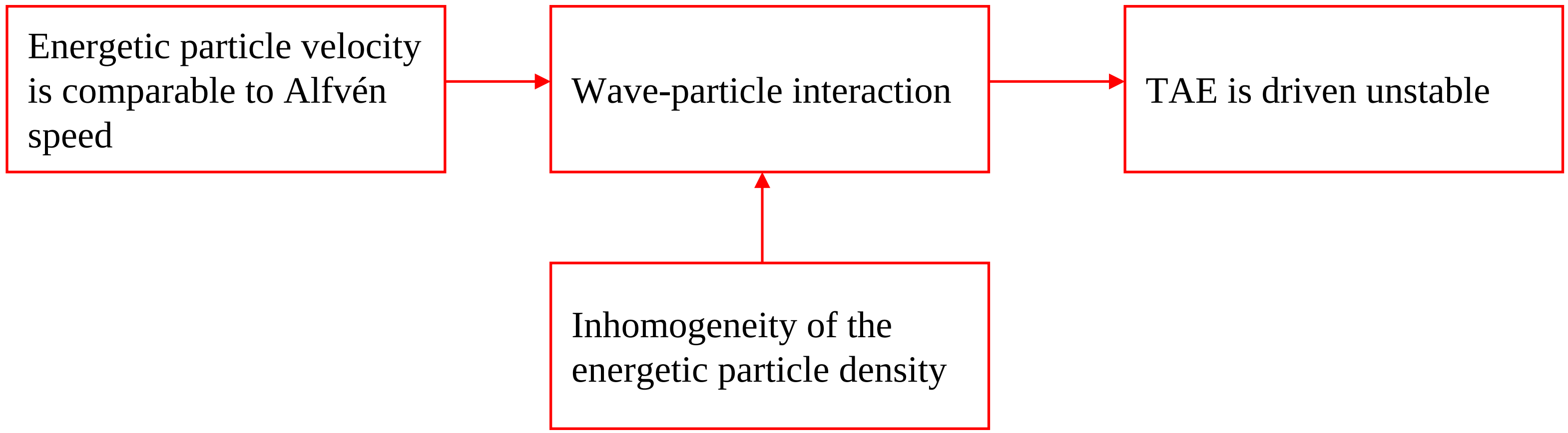

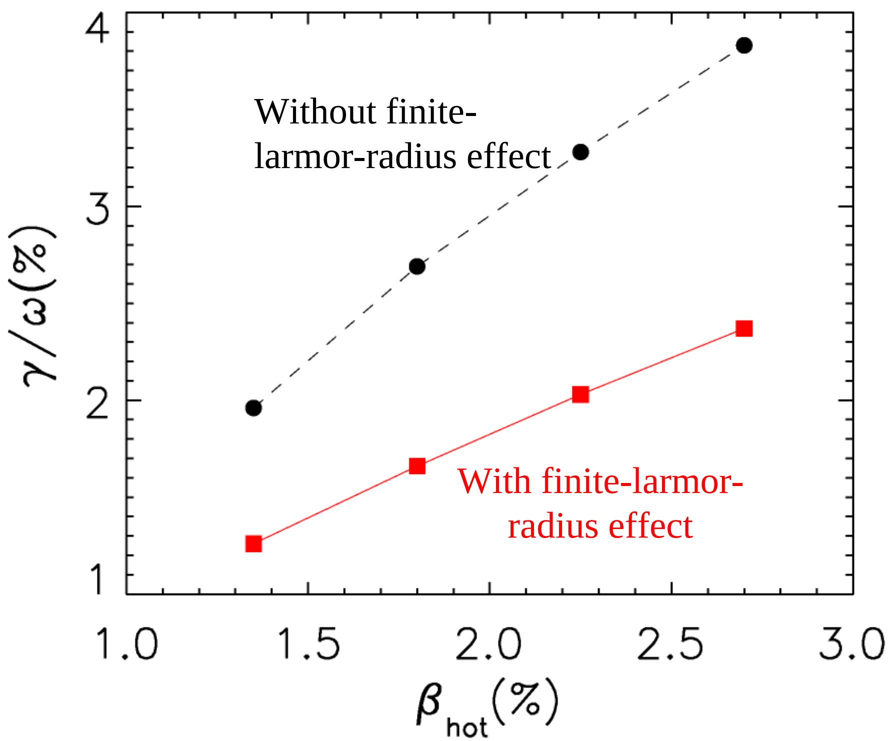

Theoretical prediction (G. Fu et al., Phys. Plasmas, 1992)

$$\frac{\gamma}{\omega} \propto q^2 \beta_{hot} \left(\frac{\omega_*}{\omega_{TAE}} - 1 \right)$$

- q is the tokamak safety factor
- β_{hot} is the energetic particle pressure to magnetic pressure ratio $\beta_{hot} \propto n_{hot} T_{hot}$
- ω_* is the diamagnetic drift frequency of energetic particle $\omega_* \propto \kappa_{hot}$

The damping of TAEs

- Thermal ion Landau damping (very small)
- Trapped electron collisional damping (neglected by fluid electron approximation)
- Radiative damping due to coupling to the kinetic Alfvén waves

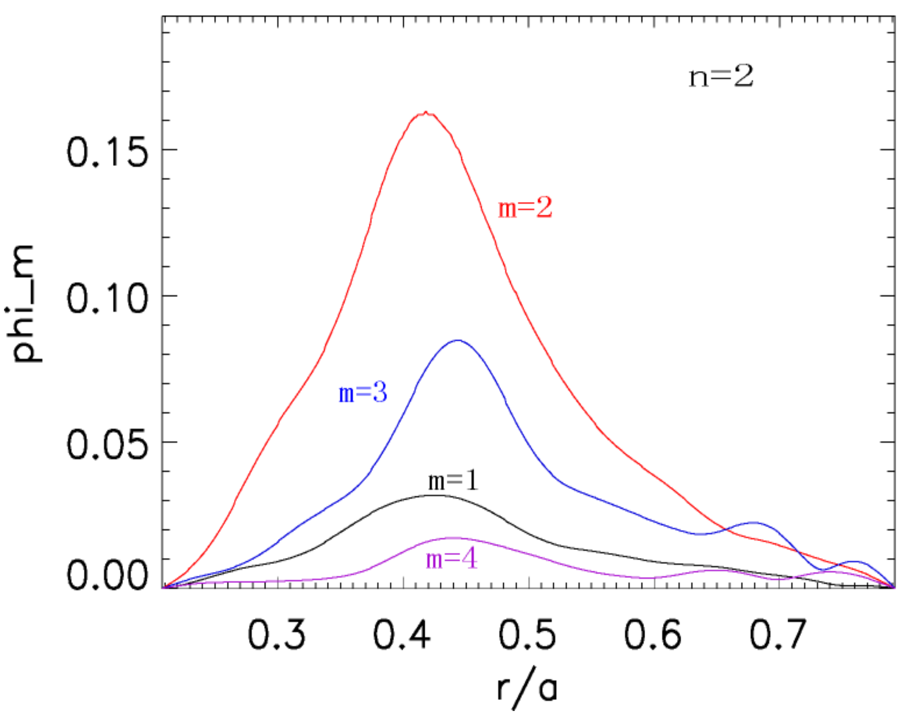

Mode structure with MHD operator

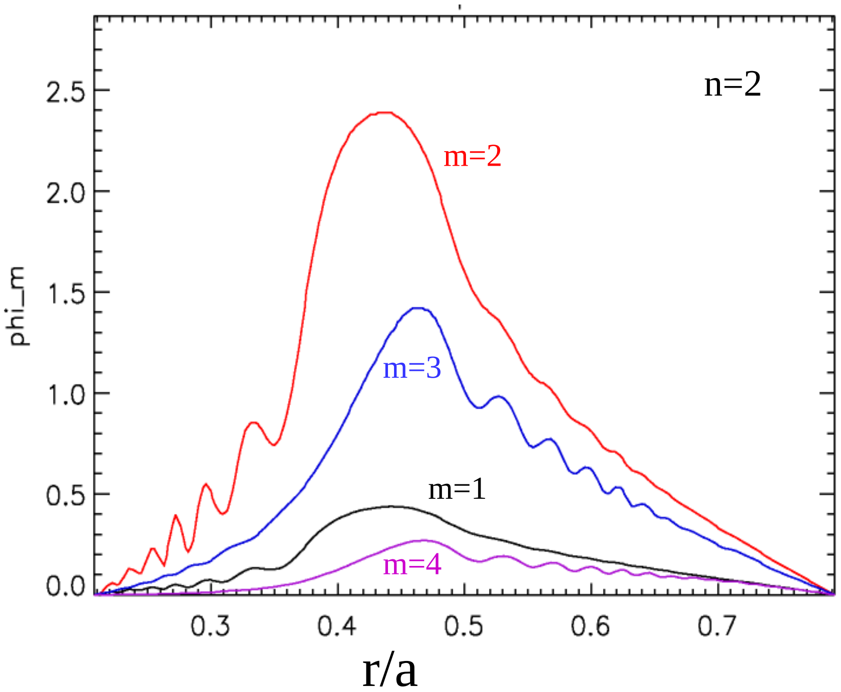

Mode structure with gyrokinetic operator

Radiative damping

Analytical calculation of the thermal ion radiative damping (Fu. et al., Phys. Plasmas, 1996)

$$\frac{\gamma_d}{\omega} \propto e^{-\frac{2}{\sqrt{\eta}} I_1(h)},$$

where $\eta = 8n^2 \hat{s}^2 q^2 \rho_i^2 / \varepsilon^3 / r_m^2$

$$I_1(h) = \int_0^{\sqrt{1+h}} \sqrt{1-(h-x^2)^2}\, dx,$$

where $h = (\omega^2 / \omega_{TAE}^2 - 1) / \varepsilon$

Damping rate increases with thermal ion larmor radius

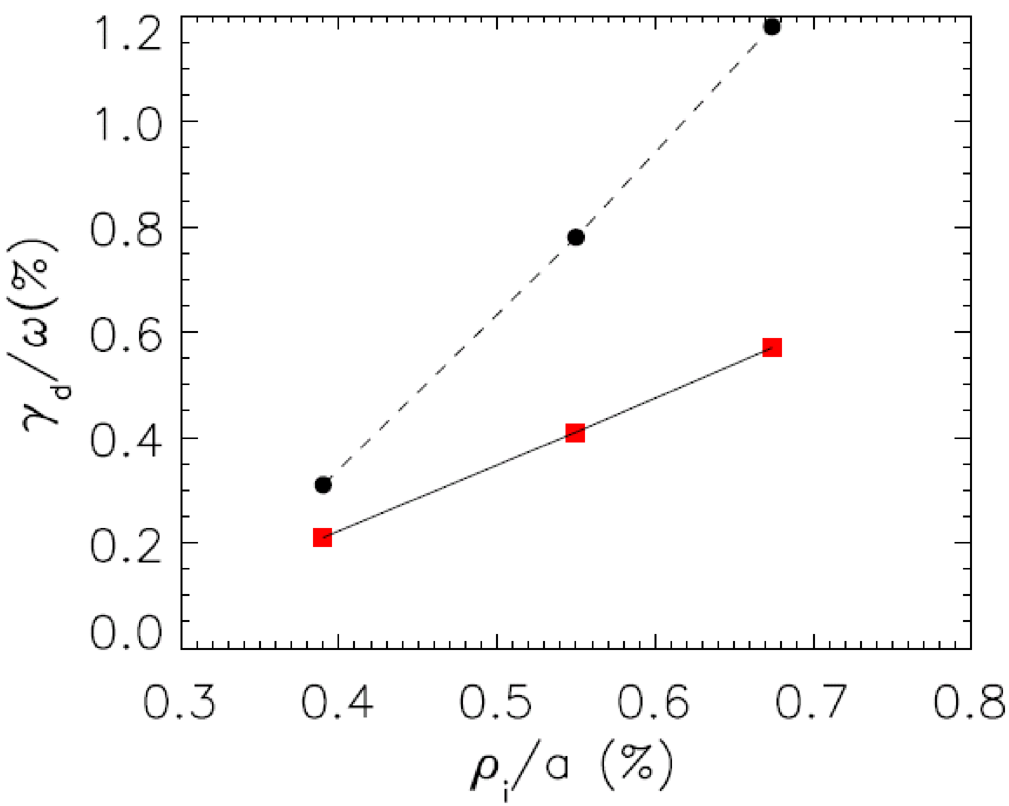

Summary and conclusion

- **The gyrokinetic code is extended to simulate MHD instabilities—TAEs**
  - The TAE mode is observed in simulations
  - The simulation results are benchmarked with an eignemode calculation in a simplified form
  - The TAE is driven unstable in the presence of energetic particles
  - Radiative damping mechanism is demonstrated in our simulations